Biochemical and Biophysical Research Communications 403 (2010) 126–132

Contents lists available at ScienceDirect

Biochemical and Biophysical Research Communications

journal homepage: www.elsevier.com/locate/ybbrc

NMR solution structure of the N-terminal domain of hERG and its interaction with the S4–S5 linker

Qingxin Li [1,2], Shovanlal Gayen [2], Angela Shuyi Chen, Qiwei Huang, Manfred Raida, CongBao Kang *

Experimental Therapeutics Center, The Agency for Science, Technology and Research, 31 Biopolis Way Nanos, #03-01, Singapore 138669, Singapore

ARTICLE INFO

Article history:
Received 13 October 2010
Available online 3 November 2010

Keywords:
Potassium channel
hERG
NMR spectroscopy
PAS domain
CD
Amphipathic helix

ABSTRACT

The human Ether-à-go-go Related Gene (hERG) potassium channel mediates the rapid delayed rectifier current (IKr) in the cardiac action potential. Mutations in the 135 amino acid residue N-terminal domain (NTD) cause channel dysfunction or mis-translocation. To study the structure of NTD, it was overexpressed and purified from *Escherichia coli* cells using affinity purification and gel filtration chromatography. The purified protein behaved as a monomer under purification conditions. Far- and near-UV, circular dichroism (CD) and solution nuclear magnetic resonance (NMR) studies showed that the purified protein was well-folded. The solution structure of NTD was obtained and the N-terminal residues 13–23 forming an amphipathic helix which may be important for the protein–protein or protein-membrane interactions. NMR titration experiment also demonstrated that residues from 88 to 94 in NTD are important for the molecular interaction with the peptide derived from the S4–S5 linker.

1. Introduction

The human Ether-à-go-go related gene (hERG) gene is primarily expressed in the heart and was originally identified from a human hippocampal cDNA library [1,2] and it was also shown to be expressed in multiple tissues and cell types including neural smooth muscle and tumor cells [3,4]. hERG plays an important role in the regulation of membrane potential by controlling the rapid delayed rectifier K^+ current (I_{Ks}) in the heart [2,3,5]. Gain- or loss-of-function mutations in hERG contribute to cardiac diseases such as short QT syndrome (SQTS) and long QT syndrome (LQTS) [6]. Distinct mutations in hERG represent at least 45% of LQTS-related mutations identified so far [6,7]. Despite the roles of hERG in causing lethal arrhythmia through inherited mutations or binding with drugs, the physiological functions and mechanism of gating this channel still remain unresolved [3].

Like other potassium channels, hERG is functional as a homotetramer with each subunit contains six transmembrane segments (S1–S6), an N-terminal region and a C-terminal tail [8]. The N-terminal region contains a Per-Arnt-Sim (PAS) domain whose structure was studied by X-ray crystallography [9]. The N-terminal PAS domain was shown to be important for the assembly and gating of hERG channel [9]. Biochemical study showed that PAS domain formed oligomer under some conditions and tetramer formation indicated that it may be important for the channel assembly [10]. Deletion of the whole N-terminus or N-terminal 135 residues (NTD, also called eag domain) increased the deactivation rate greatly [11]. Previous study proposed that the NTD regulated channel gating through its interaction with the core of the channel and the S4–S5 linker may be the binding sites [11]. This domain was also showed to be in close proximity to the core of hERG channels using fluorescence resonance energy transfer (FRET) spectroscopy and there were direct-, non-covalent interactions between NTD and the hERG channel core, that were sufficient to regulate deactivation gating of the channel [12]. The first 25 amino acids which had no structural information in the crystal study were shown to be crucial to the channel function [9]. Mutations in NTD also affected channel function, such as T65P causing HERG trafficking deficiency and F29/Y43A affecting channel deactivation [9,13].

To study the structure of the hERG NTD using solution NMR spectroscopy, it was cloned and overexpressed in *Escherichia coli* cells. CD and NMR studies showed that the purified protein was

Abbreviations: hERG, the human Ether-à-go-go Related Gene; NTD, hERG N-terminal 135 amino acids; IKr, rapid delayed rectifier current; LQTS, long QT syndrome; SQTS, short QT syndrome; TdP, torsades de pointes; PAS, Per-Arnt-Sim; EDTA, ethylenediaminetetraacetic; SDS–PAGE, sodium dodecyl sulfate polyacrylamide gel electrophoresis; HSQC, heteronuclear single quantum coherence.

* Corresponding author. Address: 31 Biopolis Way Nanos, #03-01, Singapore. Fax: +65 64788768.
E-mail address: cbkang@etc.a-star.edu.sg (C. Kang).
[1] Present address: Institute of Bioengineering and Nanotechnology, The Agency for Science, Technology and Research, Singapore 138669, Singapore.
[2] These authors contribute equally to this work.

0006-291X/$ - see front matter © 2010 Elsevier Inc. All rights reserved.
doi:10.1016/j.bbrc.2010.10.132

well-folded. We determined the protein structure using solution NMR spectroscopy. The structural information of the N-terminal 1–25 residues which was not observed in X-ray study was analyzed. NMR titration with peptide from S4–S5 linker of the channel demonstrated that the residues 88–94 from NTD are important for the interactions.

2. Materials and methods

2.1. Protein expression and purification

The sequence encoding the N-terminal 135 amino acids (NTD) of hERG was amplified using polymerase chain reaction (PCR). PCR product was inserted into pET16b plasmid to generate pET16b-NTD which encodes a fusion protein with a decahistidine tag and a Factor Xa cleavage site at the N-terminus. The plasmid was transformed into *E. coli* BL21 (DE3) codon plus RIL competent cells and cells were grown on LB plates containing both 34 μg/ml of chloramphenicol and 100 μg/ml of ampicillin. A single colony was picked and incubated in 20 ml of M9 medium with antibiotics. The overnight culture was transferred into 1 L of M9 medium with antibiotics. Induction was performed by adding IPTG to 1 mM final concentration with additional shaking at 240 rpm for 3 h at 25 °C when OD_{600} reached to 0.8. *E. coli* cells were harvested by centrifugation at 10,000*g* for 10 min at 4 °C and the cell pellets were resuspended in a lysis buffer containing 20 mM Sodium phosphate, pH 7.8, 500 mM NaCl, 2 mM β-mercaptoethanol and broken by sonication on ice. Cell lysates were cleared by centrifugation at 40,000*g* for 20 min and the supernatant was mixed with Ni^{2+}-NTA resin at 4 °C for 1 h before being passed through a column. Resin with protein was washed with at least 10 resin volumes of washing buffer containing 50 mM Sodium phosphate, pH 7.4, 1 M NaCl, 30 mM imidazole and 2 mM β-mercaptoethanol to remove unspecific proteins binding to the resin. Protein was eluted with elution buffer containing 500 mM imidazole, pH 6.5, 500 mM NaCl and 2 mM β-mercaptoethanol.

2.2. Protein purification and molecular weight determination using gel filtration

The Ni^{2+}-NTA purified protein was further purified using Superdex 200 gel filtration column equilibrated with two column volumes of purification buffer containing 20 mM Sodium phosphate, pH 6.5, 2 mM Dithiothreitol (DTT), 1 mM ethylenediaminetetraacetic acid (EDTA) and 150 mM NaCl. Purified fractions were analyzed by sodium dodecyl sulfate polyacrylamide gel electrophoresis (SDS–PAGE). To determine the molecular weight of the purified proteins, molecular weight standards were run using the same purification buffer. The elution profile of the standards was used to draw a standard curve plotting the Kav versus the log of molecular weight as described before [14].

2.3. Preparation of ^{15}N- or $^{15}N/^{13}C$- labeled samples for NMR study

Protein was uniformly ^{15}N- or $^{15}N/^{13}C$-labeled in M9 medium with 1 g/L of $^{15}NH_4Cl$ or 1 g/L $^{15}NH_4Cl$ and 2 g/L of ^{13}C-glucose. The final purified protein was concentrated using an ultra-filtration spin column (M.W cut off 3000) to a 0.5–1.0 mM final concentration and transferred into a 5 mm NMR tube for NMR analysis.

2.4. Protein digestion with protease

Ni^{2+} – NTA purified protein was exchanged into a buffer containing 20 mM Tris–HCl, pH 7.8, 2 mM DTT, 50 mM NaCl and 2 mM $CaCl_2$ using a PD10 desalting or gel filtration column. The digestion was performed at room temperature for at least 24 h to obtain complete digestion. The digested products were run through Superdex 200 column to remove the protease and cleaved fusion tag.

2.5. Circular dichroism (CD) spectroscopy

Far-UV spectrum of the protein at a concentration of 0.3 mg/ml was analyzed in a buffer containing 20 mM sodium phosphate, pH 6.5, 150 mM NaCl, 2 mM β-mercaptoethanol. The instrument was blanked using a cuvette containing buffer without protein. The CD spectra were recorded on a Jasco J-810 instrument at 25 °C and samples were placed in a 0.1-cm path length quartz cuvette. Protein at a concentration of 2 mg/ml in a quartz cuvette with a 1-cm path length was used for the near-UV analysis. The results were then analyzed using CDNN (http://www.photophysics.com/cdnn.php).

2.6. NMR spectroscopy and structure determination

Proteins were purified to a final concentration of 0.5–1.0 mM in a buffer containing 20 mM Sodium phosphate, pH 6.5, 5 mM DTT, 1 mM EDTA, 150 mM NaCl, 10% D_2O. All the NMR experiments were conducted at 298 K. A one dimensional (1D) proton spectrum was recorded, processed and visualized with Topspin 1.3. The protein backbone and side chain assignments were performed as described before [15]. Distance restraints were from ^{15}N- and ^{13}C-edited NOESY spectra with a mixing time of 100 and 120 ms. Peaks were picked in Sparky (http://www.cgl.ucsf.edu/home/sparky/) and automated NOE cross-peak assignment was performed using CYANA [16] and the auto-assigned peaks were manually checked. The dihedral angles were from TALOS+ [17] and the hydrogen bond were obtained based upon TALOS+ and NOE analysis. Structures were validated using the PROCHECK [18]. The spectra were processed with NMRPipe [19] and visualized with NMRView [20].

2.7. NMR titration

Titration between protein and peptide was conducted at Bruker Avance magnet with 600 MHz proton Larmor frequency. Peptide sequence from S4–S5 linker was based upon the sequence analysis from the uniprot server (http://www.uniprot.org/uniprot/Q12809). Peptide sequence is RYSEYGAAV with 97% purity, which was purchased from GL Biochem. Peptide was dissolved in water to 15 mM concentration. Aliquots of peptide were added to ^{15}N labeled NTD and HSQC spectra were acquired.

3. Results

3.1. Protein purification from E. coli cells

The ^{15}N and $^{15}N/^{13}C$-labeled NTD with an N-terminal tag were first purified from lysate supernatants (Fig. 1A) using Ni^{2+}-NTA resin. The recombinant protein was further purified using gel filtration chromatography. After gel filtration, the purified protein was then cleaved with Factor Xa to remove the N-terminal decahistidine tag and the NTD was separated from the cleavage tag by a second gel filtration step (Fig. 1A, lane 7). After Ni^{2+}-NTA affinity column and two rounds of gel filtrations, a homogenous protein was obtained (Fig. 1A, lane 7). Both NTD with and without an N-terminal tag had very similar retention volumes of ~17 ml corresponding to a protein with a molecular weight of ~16 kDa protein (Fig. 1B) which was close to its theoretical mass (~17 kDa). The purified proteins were confirmed by mass spectroscopy (MS) analysis and Western blot (Fig. S1).

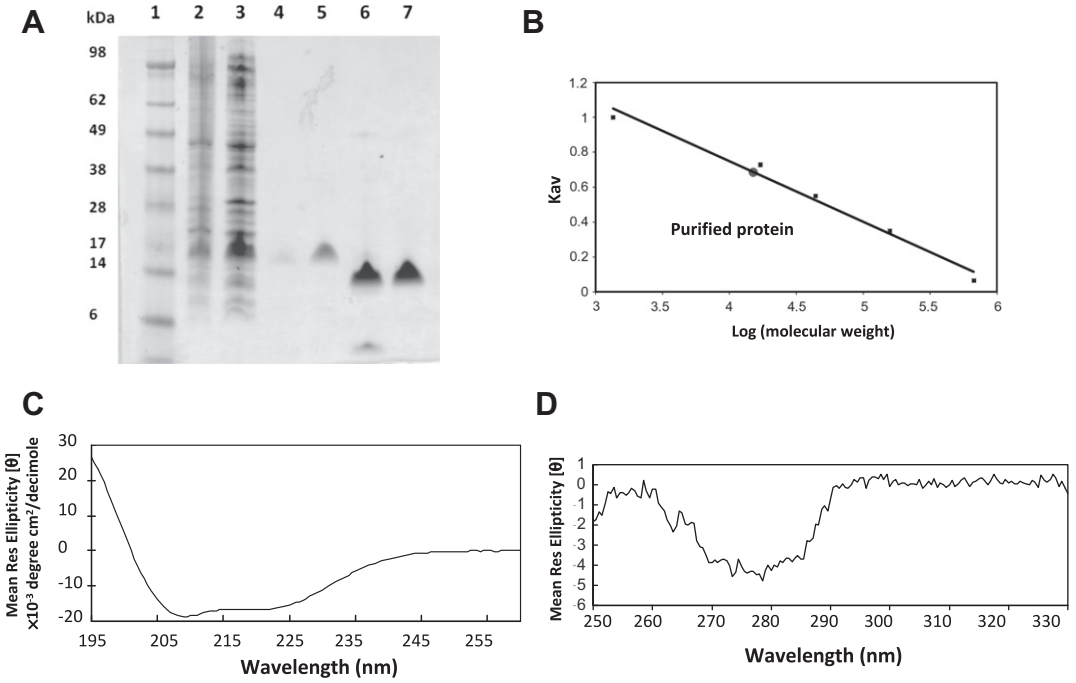

Fig. 1. (A) Purification of the NTD from *E. coli* cells. A. SDS–PAGE analysis of purification of the NTD. The lanes of the gel were as follows: 1, molecular weight standard; 2, the cell lysate; 3, the supernatant which was loaded onto the column; 4, the cell pellet resuspended in the same volume of lysis buffer. 5, an elution fraction from the Ni^{2+}-NTA column; 6, purified protein digested with Factor-Xa protease; 7, final purified NTD after protease digestion. (B) Molecular weight analysis using gel filtration. The diamond symbols are the protein molecular weight standards. The cycle symbol was the NTD. Kav = $(V_e–V_0)/(V_t–V_0)$. V_e was the retention volume of the protein sample. Values for void volume (V_0) and total volume (V_t) were as follows: V_0 = 9.8 ml and V_t = 26.5 ml. (C and D) Far-UV and near-UV spectra of the NTD.

3.2. CD spectra of purified protein

Far-UV spectrum of NTD (Fig. 1C) showed ~20% alpha-helical and ~39% beta-sheet structures present, which was similar to the crystal structure. Near-UV signals from the side chains of aromatic amino acids and disulfide bonds were also measured (Fig. 1D). The signals from side chains of tyrosine and phenylalanine were observed at 270–290 and 260–270 nm. No tryptophan signal was observed at 280–300 nm which was consistent with that there was no tryptophan present in the protein sequence. Both near-UV and far-UV spectra showed that purified protein was folded into a well-defined structure.

3.3. NMR spectra

In 1D proton NMR spectra, the dispersion of the NMR signals in the regions of the methyl protons, α-protons, and amide protons was the main indicator of folded globular proteins [21]. Both NTD with and without an N-terminal tag showed very well-dispersed peaks in both amide proton regions and methyl group regions indicating that they were well folded (Fig. S2). Both proteins had well-dispersed ^{1}H-^{15}N-HSQC spectra (Fig. S3), which further confirmed their well-folded structure. There was no obvious chemical shift perturbation observed for NTD with and without the N-terminal tag (Fig. S3). The backbone assignment of the NTD with an N-terminal tag was achieved from the 3D HNCACB, CBCACOHN and HNCA experiments. There are 151 expected cross peaks in the ^{1}H-^{15}N-HSQC spectrum (5 prolines) and ~136 out of 151 (21 of them were from N-terminal tag) backbone amide and amine protons were assigned (Fig. S3). The backbone and side chain assignments of the NTD only and this domain with a C-terminal histidine tag were completed [22,23].

Secondary structure analysis of NTD with an N-terminal tag was performed using Chemical Shift Index (CSI) based upon the Ca chemical shifts [24]. Analysis showed that residues 26–135 consisted of 3 alpha-helical and 5 beta-sheet regions, which was consistent with the crystal structure (Fig. S3B) [9] and NMR analysis using TALOS+ [22,23]. All the NMR studies showed the presence of an alpha-helical fragment (residues 13–23) which was not observed in the study of X-ray crystallography [9].

3.4. Structure determination

The solution structure of the NTD was determined by heteronuclear triple-resonance NMR spectroscopy using double labeled ($^{13}C/^{15}N$) samples. The structures were determined based upon 1591 experimental restraints including interproton distances, dihedral angles and hydrogen bonds. Table 1 gives the structural and restraint statistics of the 20 lowest energy minimized structures. Fig. 2A and B shows an overlay of the ensemble structures obtained with CYANA. The pair wise RMSD for the residues 27–132 of the ensemble of 20 structures is 0.83 Å. The atomic coordinates for all 20 structures have been deposited in the Protein Data Bank with the accession number of 2L4R. Like other PAS domain, solution structure of this domain showed a highly conserved α/β fold (Fig. 2C and D). The residues 26–135 contain a five-stranded anti-parallel β-sheet hanged around a long helical connector and a bundle of two small helices. The strand order is βC–βD–βE–βA–βB for the PAS core, in which the βA and βE are from N- and C-terminus of NTD (Fig. 2C). The five strands are βA (resides 27–33), βB (resides 42–44), βC (resides 90–99), βD (resides 105–116), βE (resides 122–132) and α-helices are αA (resides 46–52), αB (resides 56–60), αC (resides 75–86) (Fig. 2C and D). The reported crystal structure contains the coordinate of the PAS domain (residues 26–135) in which there is a 3_{10} helix (α′A) containing residues 67–69 [9]. TALOS+ analysis showed that only residues 67 and 68 form helical structure. The superposition of the NMR structure onto the crystal structure of NTD gives an RMSD for the protein

Table 1
Statistics for the 20 final structural models of NTD.

Total number of NMR restraints	1591
Number of unambiguous NOEs	
Intraresidual ($\|i-j\| = 0$)	635
Short range ($\|i-j\| \leqslant 1$)	415
Medium-range ($2 \leqslant \|i-j\| \leqslant 5$)	128
Long-range ($\|i-j\| > 5$)	159
Number of dihedral angle constraints	216
Number of hydrogen-bond restraints	38
Number of restraint violations[a]	
Total number of restraint violations >0.5 Å	0
Total number of dihedral angle constraints >5°	0
Ramachandran plot statistics[b] *(%)*	
Residues in most favoured regions	78.9
Residues in additionally allowed regions	19.7
Residues in generously allowed regions	1.4
Residues in disallowed regions	0
Average RMSD to mean (Å)	
Backbone (residues 27–132)	0.83 ± 0.17 Å
Heavy atoms (residues 27–132)	1.51 ± 0.20 Å

[a] There are no distance violations greater than 0.5 Å or dihedral angle violations greater than 5°. All residues are included in the final ensemble.
[b] The Ramachandran plot was for all the residues.

backbone atoms (N, Ca and C′) of 1.2 Å for residues from 26 to 135. Fig. 2B shows the comparison of the two structures (residues 26–135), indicating their structural similarity. The crystal structure does not have the coordinate of residues 1–25 may due to the mobility of this fragment.

3.5. The residues 13–23 form an amphipathic helix

The residues 13–23 form one α-helical structure which is donated as αA′ to conform to the naming scheme for the secondary structural elements in PAS domains. There is no unambiguous long-range NOE identified between this helix and other regions, which may be the reason that this domain was not modeled in its crystal structural study even though some electron density was observed [9]. The N-terminal 1–25 residues were shown to be important for regulation of the channel function and deletion of these residues results in greatly increased rate of deactivation [9]. Analysis on these residues showed that αA′ formed an amphipathic helix (Fig 3A). The segregation of hydrophobic residues (F14, L15, I18, I19 and F22) and polar residues at the two opposite faces were observed in αA′ (Fig. 3B and C). Thus, the presence of this amphipathic helix in the N-terminal 1–25 residues may explain its role in channel regulation.

3.6. Binding study between NTD and S4–S5 linker

The NTD was proposed to interact with the S4–S5 linker [9,11,12]. With the backbone assignment, we tested the possible interaction with the linker peptide. The perturbations of chemical shifts in HSQC experiments were monitored after the addition of

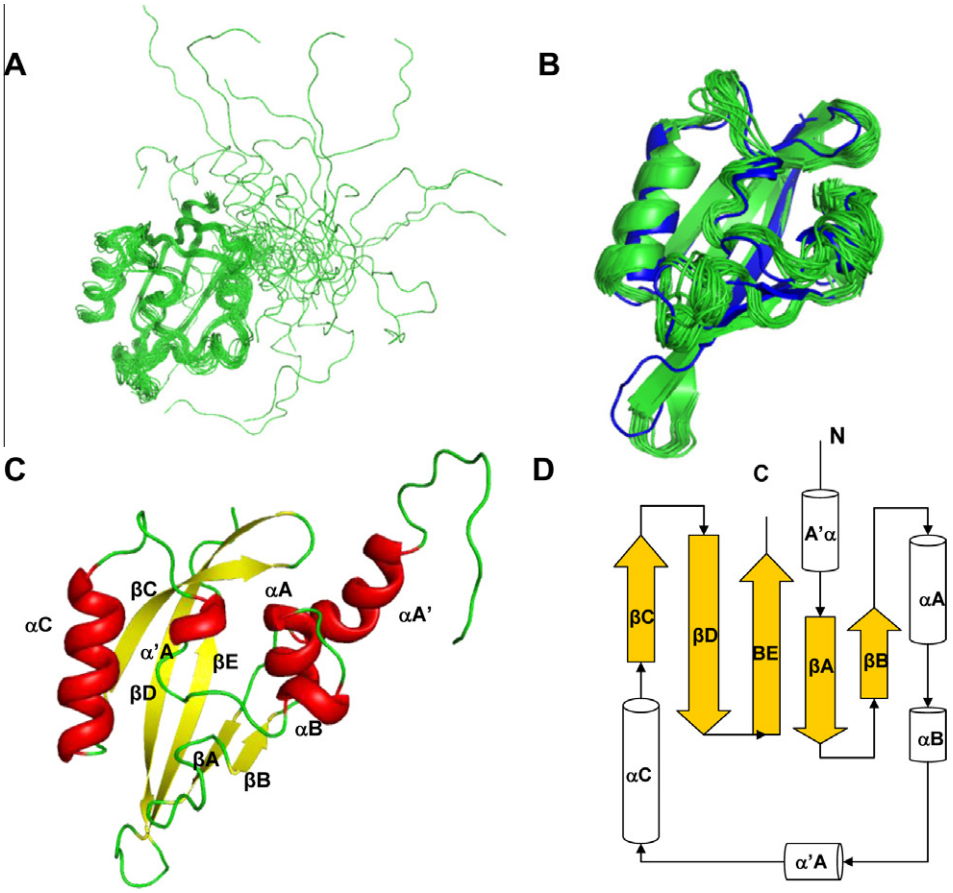

Fig. 2. NMR structure of NTD. (A) Ensemble of the 20 structures after water refinement with Ca trace only (B) Superimposed NMR and X-ray structures. The X-ray structure (pdb: 1byw) is shown in blue and NMR structures are shown in green. The residues 1–25 was removed in the NMR structures. (C) Ribbon representation of one solution structure of NTD. The structure is shown with pymol. (D) Topology diagram of the NTD structure. The beta-sheet is shown in arrow and the alpha structure was shown in cylinder (For interpretation of the references to colour in this figure legend, the reader is referred to the web version of this article.).

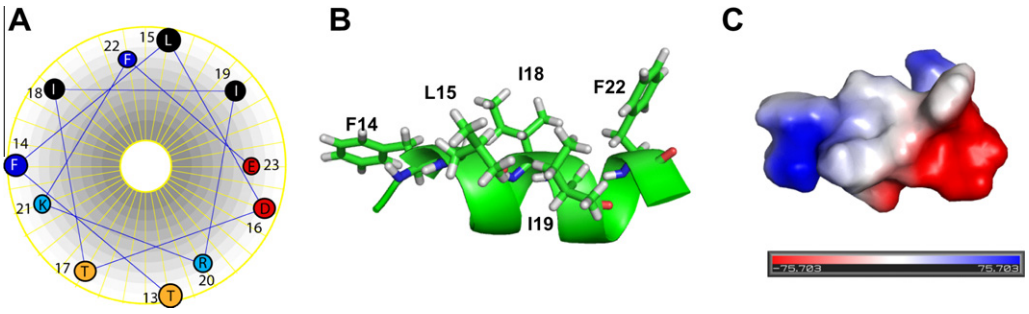

Fig. 3. Structure of residues 13–23. (A) Helix wheel representation of residues 13–23. Residues M, L, I and V are shown in black, F in blue, D and E in red, S and T in brown. (B) Structure of residues 13–23. Hydrophobic residues are shown in sticks mode. (C) Electrostatic potential surface presentation of residues 13–23 using pymol (www.pymol.org) (For interpretation of the references to colour in this figure legend, the reader is referred to the web version of this article.).

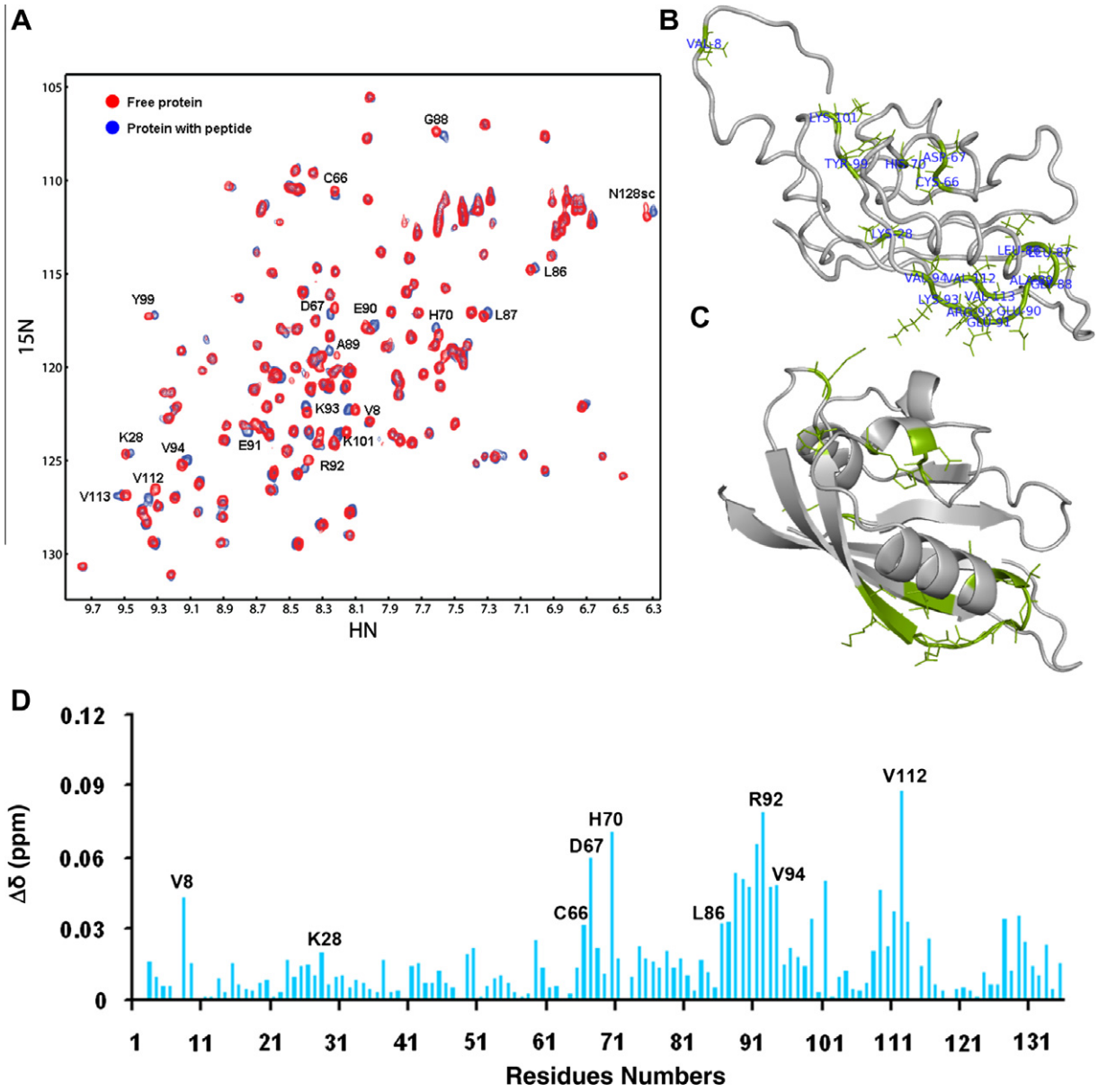

Fig. 4. Titration between NTD and peptide derived from S4–S5 linker. (A) Superimposed HSQC spectra of NTD in the presence and absence of peptide. The NTD with 0.3 mM concentration was mixed with peptide with final concentration of 2 mM. (B) Residues affected when NTD was titrated with peptide in the NMR structure. (C) Residues affected were mapped to the crystal structure (pdb: 1byw) in the same view as in (B). (D) Chemical shift changes versus residue numbers upon peptide was mixed with ^{15}N labeled protein.

the peptide (Fig. 4A). Chemical shift perturbations of several residues were observed (Fig. 4A). The most affected ones including residues 66–67, 70, 86–94 and 112–113, were summarized in Fig. 4B–D. The affected residues were mapped to both NMR and crystal structures (Fig. 4B–C). As resides 86–94 are located between αC and βC which are easily accessible, these resides were predicted to be the main binding sites for the peptide.

4. Discussion

The N-terminus was important for the regulation of hERG potassium channel and deletion of this region caused the increased rate of deactivation [25]. In this study, the N-terminus was overexpressed and purified from *E. coli* cells with a histidine tag. CD results showed that the purified protein was well folded. Purified proteins have nicely dispersed NMR signals allowing us to perform resonance assignment and structure determination. This domain was shown to form an oligomer under some conditions and may be important for the channel assembly through this oligomerization [10]. Under our purification conditions, the recombinant proteins were shown to be a monomer from the gel filtration analysis (Fig. 1B). With purified proteins and assignment of NMR spectra, it is possible to perform the protein oligomerization study to understand its role in channel regulation.

NTD was confirmed to be a PAS domain from the reported X-ray crystallography study [9]. Our NMR structure showed the similar structure of residues 26–135 to that of X-ray. However, the first 25 amino acids having no structural information in the crystal structure were also characterized in our study. Residues 13–23 were shown to form an alpha helical (αA′) structure. There was no unambiguous long-range NOE identified between αA′ and the other regions. The missing of long-range NOEs in NMR study and electron density in X-ray study of these residues may due to its possible multiple conformations which may be important for its interactions with the body of channel as proposed under some conditions [9].

The amphipathic helix in protein plays important roles in binding with cell membrane. A model amphipathic helix adopts an orientation parallel to the membrane plane with its hydrophobic residues inserting between fatty acyl-chains [26]. The amphipathic helix was also found in some PAS domain containing proteins and the helix was responsible for the dimmerization [27,28]. We also found that the αA′ which was not modeled in X-ray study has the characteristics of an amphipathic helix with hydrophobic residues facing in one side and hydrophilic ones facing in another. The existence of this amphipathic helix may be important for the function of NTD through its interaction with other proteins or with the cell membrane. A study showed that deletion of the first 26 resides at the N-terminus had different effect on channel deactivation rate from the deletion of the first 9 residues [9], which indicates that amphipathic helix (13–23) may play important roles in channel regulation. Detailed study on this amphipathic helix in membrane mimicking environment and with more experimental restraints such as residue dipolar coupling will provide more structural insight to understand the role of this amphipathic helix in channel regulation.

It was also proposed the N-terminal residues of NTD may interact with the S4–S5 linker [9]. Titration study demonstrated there were interactions between NTD and the peptide derived from this linker. The residues involved in the interaction with peptide were mainly present in the region containing resides 86–94. The interaction between NTD and peptide was observed in our NMR study indicating that the S4–S5 linker may play important roles in the channel gating through interaction with the NTD. The further work will be the interaction study between the peptide and protein in membrane mimicking environment to better understand the interaction mechanisms.

In summary, we obtained the N-terminal domain of hERG containing 135 residues from *E. coli* cells and its NMR structure was shown to be similar to that of X-ray. Our NMR study on the 1–25 residues showed a complementary result to the crystal study, which will provide a structural basis to understand its role in the channel regulation. The N-terminal 25 residues contain an α-helix with amphipathic characteristics, which may be important for protein–protein or protein–membrane interactions. Our NMR titration supported the hypothesis that the S4–S5 linker is important for the interaction with this domain.

Acknowledgments

C.K. appreciates the financial support from the Agency for Science, Technology and Research (A*STAR), Singapore. C.K. is a recipient of A*STAR Investigatorship. We thank the support from Prof. Charles R. Sanders in Vanderbilt University and Prof. Ho Sup Yoon in Nanyang Technological University. We also thank Ms. Ee Kim Huey for protein identification.

Appendix A. Supplementary data

Supplementary data associated with this article can be found, in the online version, at doi:10.1016/j.bbrc.2010.10.132.

References

[1] J.W. Warmke, B. Ganetzky, A family of potassium channel genes related to eag in *Drosophila* and mammals, Proc. Natl. Acad. Sci. USA 91 (1994) 3438–3442.
[2] M.E. Curran, I. Splawski, K.W. Timothy, G.M. Vincent, E.D. Green, M.T. Keating, A molecular basis for cardiac arrhythmia: HERG mutations cause long QT syndrome, Cell 80 (1995) 795–803.
[3] M.C. Sanguinetti, M. Tristani-Firouzi, HERG potassium channels and cardiac arrhythmia, Nature 440 (2006) 463–469.
[4] J.H. Dolderer, H. Schuldes, H. Bockhorn, M. Altmannsberger, C. Lambers, D. von Zabern, D. Jonas, H. Schwegler, R. Linke, U.H. Schroder, HERG1 gene expression as a specific tumor marker in colorectal tissues, Eur. J. Surg. Oncol. 36 (2010) 72–77.
[5] M.C. Sanguinetti, C. Jiang, M.E. Curran, M.T. Keating, A mechanistic link between an inherited and an acquired cardiac arrhythmia: HERG encodes the IKr potassium channel, Cell 81 (1995) 299–307.
[6] E. Raschi, V. Vasina, E. Poluzzi, F. De Ponti, The hERG K+ channel: target and antitarget strategies in drug development, Pharmacol. Res. 57 (2008) 181–195.
[7] I. Splawski, J. Shen, K.W. Timothy, M.H. Lehmann, S. Priori, J.L. Robinson, A.J. Moss, P.J. Schwartz, J.A. Towbin, G.M. Vincent, M.T. Keating, Spectrum of mutations in long-QT syndrome genes. KVLQT1, HERG, SCN5A, KCNE1, and KCNE2, Circulation 102 (2000) 1178–1185.
[8] M.J. Perrin, R.N. Subbiah, J.I. Vandenberg, A.P. Hill, Human ether-a-go-go related gene (hERG) K(+) channels: function and dysfunction, Prog. Biophys. Mol. Biol. (2008).
[9] J.H. Morais Cabral, A. Lee, S.L. Cohen, B.T. Chait, M. Li, R. Mackinnon, Crystal structure and functional analysis of the HERG potassium channel N terminus: a eukaryotic PAS domain, Cell 95 (1998) 649–655.
[10] X. Li, J. Xu, M. Li, The human delta1261 mutation of the HERG potassium channel results in a truncated protein that contains a subunit interaction domain and decreases the channel expression, J. Biol. Chem. 272 (1997) 705–708.
[11] J. Wang, M.C. Trudeau, A.M. Zappia, G.A. Robertson, Regulation of deactivation by an amino terminal domain in human ether-a-go-go-related gene potassium channels, J. Gen. Physiol. 112 (1998) 637–647.
[12] A.S. Gustina, M.C. Trudeau, A recombinant N-terminal domain fully restores deactivation gating in N-truncated and long QT syndrome mutant hERG potassium channels, Proc. Natl. Acad. Sci. USA 106 (2009) 13082–13087.
[13] A. Paulussen, A. Raes, G. Matthijs, D.J. Snyders, N. Cohen, J. Aerssens, A novel mutation (T65P) in the PAS domain of the human potassium channel HERG results in the long QT syndrome by trafficking deficiency, J. Biol. Chem. 277 (2002) 48610–48616.
[14] H.R. Yoon, C.B. Kang, J. Chia, K. Tang, H.S. Yoon, Expression, purification, and molecular characterization of *Plasmodium falciparum* FK506-binding protein 35 (PfFKBP35), Protein Expr. Purif. 53 (2007) 179–185.
[15] Q. Li, M. Raida, C. Kang, ^{1}H, ^{13}C and ^{15}N chemical shift assignments for the N-terminal domain of the voltage-gated potassium channel-hERG, Biomol. NMR Assign. 4 (2010) 211–213.
[16] P. Guntert, Automated NMR structure calculation with CYANA, Methods Mol. Biol. 278 (2004) 353–378.

[17] Y. Shen, F. Delaglio, G. Cornilescu, A. Bax, TALOS+: a hybrid method for predicting protein backbone torsion angles from NMR chemical shifts, J. Biomol. NMR 44 (2009) 213–223.
[18] R.A. Laskowski, J.A. Rullmannn, M.W. MacArthur, R. Kaptein, J.M. Thornton, AQUA and PROCHECK-NMR: programs for checking the quality of protein structures solved by NMR, J. Biomol. NMR 8 (1996) 477–486.
[19] F. Delaglio, S. Grzesiek, G.W. Vuister, G. Zhu, J. Pfeifer, A. Bax, NMRPipe: a multidimensional spectral processing system based on UNIX pipes, J. Biomol. NMR 6 (1995) 277–293.
[20] B.A. Johnson, Using NMRView to visualize and analyze the NMR spectra of macromolecules, Methods Mol. Biol. 278 (2004) 313–352.
[21] R. Page, W. Peti, I.A. Wilson, R.C. Stevens, K. Wuthrich, NMR screening and crystal quality of bacterially expressed prokaryotic and eukaryotic proteins in a structural genomics pipeline, Proc. Natl. Acad. Sci. USA 102 (2005) 1901–1905.
[22] F.W. Muskett, J.S. Mitcheson, Resonance assignment and secondary structure prediction of the N-terminal domain of hERG (Kv11.1), Biomol. NMR Assign. (2010).
[23] Q. Li, M. Raida, C. Kang, (1)H, (13)C and (15)N chemical shift assignments for the N-terminal domain of the voltage-gated potassium channel-hERG, Biomol. NMR Assign. (2010).
[24] D.S. Wishart, B.D. Sykes, F.M. Richards, The chemical shift index: a fast and simple method for the assignment of protein secondary structure through NMR spectroscopy, Biochemistry 31 (1992) 1647–1651.
[25] R. Schonherr, S.H. Heinemann, Molecular determinants for activation and inactivation of HERG, a human inward rectifier potassium channel, J. Physiol. 493 (Pt 3) (1996) 635–642.
[26] G. Drin, B. Antonny, Amphipathic helices and membrane curvature, FEBS Lett. 584 (2010) 1840–1847.
[27] A. Moglich, R.A. Ayers, K. Moffat, Addition at the molecular level: signal integration in designed Per-ARNT-Sim receptor proteins, J. Mol. Biol. 400 (2010) 477–486.
[28] A. Moglich, R.A. Ayers, K. Moffat, Structure and signaling mechanism of Per-ARNT-Sim domains, Structure 17 (2009) 1282–1294.